THE ASTROPHYSICAL JOURNAL, 326:84–100, 1988 March 1

GASDYNAMICAL CALCULATIONS OF PREFERRED PLANES IN PROLATE AND TRIAXIAL GALAXIES. II. THE CASE OF A TUMBLING POTENTIAL

ASAO HABE
Department of Physics, Hokkaido University
AND
SATORU IKEUCHI
Tokyo Astronomical Observatory, University of Tokyo
Received 1986 September 5; accepted 1987 August 25

ABSTRACT

The gas motion in a prolate or a triaxial potential with figure rotation ("tumbling") is calculated by a "smoothed particle" method in order to investigate whether or not the gas settles into the preferred plane, which is predicted by single-particle orbit studies. A rotating gas ring or a rotating gas disk is initially assumed to be tilted to the major axis of a logarithmic-type potential which tumbles about the shortest axis. The tumbling frequency ω_t is assumed to be $\omega_{p0} \lesssim \omega_t \lesssim 2\omega_0$, where ω_{p0} is the precession frequency in the case of nontumbling potential and ω_0 is the gas rotation frequency.

At first, the gas ring precesses as a whole and is gradually deformed due to the nonsphericity of the gravitational potential. The gas ring precesses differentially, and irregular motions of gas particles are excited. Finally the gas particles collide with each other supersonically, and their irregular motions are dissipated by a shock wave. The final fates of gas rings are different depending on the initial direction of the angular momentum vector, the potential shape, and the gas rotation sense, i.e., prograde or retrograde. One of the interesting results is that a retrograde gas disk settles into the warped preferred plane within a few $\times 10^9$ yr, as predicted by single-particle orbital investigations. These results can explain the dynamics of warped dust lanes in elliptical galaxies and warped rings in polar ring galaxies. Another interesting result is that the gas finally concentrates into the galactic center in the case of a prograde or retrograde ring in a prolate or triaxial potential with sufficient elongation. This result may account for the process by which gas with angular momentum is supplied to the galactic center.

The time it takes gas to settle into the preferred plane is found to be on the order of the period of differential precession. The final warping gas plane is well described by the approximate solution of Steiman-Cameron and Durisen.

Subject headings: galaxies: internal motions — galaxies: structure — hydrodynamics

I. INTRODUCTION

Questions about the configuration of the mass distributions in galaxies have arisen from many observational results. For example, in the case of elliptical galaxies the observed rotation velocities of stars are generally too small, by a large factor, to support the observed flattening of systems (Illingworth 1977; Binney 1978, 1982). Then, since the elliptical galaxies cannot be supported by rotation, axial symmetry of the mass distribution is not expected *a priori*. The apparent twisting on the sky of the isophotal brightness contours in many elliptical galaxies is consistent with, and perhaps most easily explained by, triaxial density distributions (Williams and Schwarzschild 1979*a*, *b*; Leach 1981).

To investigate the true structure of galaxies, it has been proposed that one utilizes the preferred planes into which gas settles preferentially. Tohline, Simonson, and Caldwell (1982) indicated that a rotating gas disk in a static prolate potential precesses differentially around the symmetric axis of the potential and finally settles into the equatorial plane due to the dissipative property of gas. In a triaxial potential with figure rotation (hereafter we call this a tumbling triaxial potential), Heisler, Merritt, and Schwarzschild (1982) studied particle orbits and found stable, retrograde anomalous orbits in planes which are not perpendicular to the rotation axis of the potential. These stable, retrograde anomalous orbits tilt with respect to the rotation axis of the potential with different angles at different radii. Warped dust lanes are observed in many elliptical galaxies (Hawarden *et al.* 1981; Sharples *et al.* 1983). van Albada, Kotanyi, and Schwarzschild (1982) applied their analytical result to the warped dust lane observed in NGC 5128 and proposed that this galaxy has a prolate potential tumbling around the axis perpendicular to the major axis of the potential. Durisen *et al.* (1983) studied analytically the precession trajectories of circular orbits in a spheroidal potential. Steiman-Cameron and Durisen (1984) studied analytically the precession trajectories of circular orbits in a tumbling triaxial galaxy. They showed that there are several stable orbits depending on the directions of the tumbling axis and of the angular momentum vector of a particle, and that neighboring orbital planes precess around each stable orbit. They concluded that these stable orbits are preferred planes.

In all the works cited above, the particle motions in a given potential were followed, and the stability of orbits was examined. In order to compare the theoretical work with observations, however, it is important to investigate the realistic gas motion in a prolate or a triaxial potential. Habe and Ikeuchi (1985, hereafter Paper I) have presented numerical studies of gas motions in a prolate or a triaxial potential for the case without tumbling. It is concluded in Paper I that a tilted gas ring precesses around the symmetry axis in a prolate potential

and around the longest or shortest axis in a triaxial potential, and the gas settles into the plane perpendicular to these axes within a time during which the neighboring orbital planes of the gas precess around each stable orbit for a few precession periods. In this paper, we present our numerical study of gas motions in a prolate or a triaxial potential for the case with tumbling and try to confirm the preferred planes, especially the anomalous preferred planes.

In § II, the model of the galaxy potential and the numerical method for following the gas motion are summarized. In §§ III and IV, the numerical results of a prolate and a triaxial potential are presented, respectively. In § V, the gas settling time into a preferred plane is examined as well as the shape of the preferred plane. In § VI, comparison with observations and some discussion are presented.

II. MODELS AND NUMERICAL METHOD

a) *Model Galaxy*

We take a logarithmic potential for a prolate or a triaxial galaxy (Richstone 1980), which is written as

$$\Phi(x, y, z) = \Phi_c \ln\left[\left(\frac{x}{a}\right)^2 + \left(\frac{y}{b}\right)^2 + \left(\frac{z}{c}\right)^2 + d\right], \quad (1)$$

with

$$\Phi_c = 4\pi G\rho_c\left\{2\left[\left(\frac{1}{a}\right)^2 + \left(\frac{1}{b}\right)^2 + \left(\frac{1}{c}\right)^2\right]\right\}^{-1} d\,. \quad (2)$$

Parameters of models discussed below are for the prolate case: $a = 200$ pc, $b = c = 150$ pc: $a = 200$ pc, $b = c = 160$ pc; and $a = 200$ pc, $b = c = 170$ pc; and for the triaxial case $a = 200$ pc, $b = 160$ pc, $c = 150$ pc, or $a = 200$ pc, $b = 180$ pc, $c = 150$ pc, with $d = \exp(1) = 2.7183$ and $\rho_c = 62.5\ M_\odot\ \mathrm{pc}^{-3}$. The angular velocity of the circular motion in a spherical potential with $a = b = c = 200$ pc at $r = 5$ kpc is $\omega_0 = 2\pi \times 10^{-8}\ \mathrm{yr}^{-1}$. The angular velocity of rigid body rotation of a galaxy, ω_t, is called the tumbling rate, and we assume that ω_t is $2\pi \times 10^{-9}\ \mathrm{yr}^{-1}$, $4\pi \times 10^{-9}\ \mathrm{yr}^{-1}$, or $4\pi \times 10^{-8}\ \mathrm{yr}^{-1}$.

b) *Numerical Method*

In order to calculate the three-dimensional gas motion in a tumbling prolate or a tumbling triaxial potential, we use the so-called smoothed-particle method, which was developed by Lucy (1977), Gingold and Monaghan (1977, 1982, 1983), and Wood (1981). Our treatment is essentially the same as the references cited above and is described in Paper I. We assume the gas to be isothermal ($T = 10^4$ K). We calculate the gas motion in a rotating frame which corotates with the tumbling potential.

c) *Initial Condition*

We take as an initial state a rotating gas ring or disk with a definite angular momentum vector $\boldsymbol{L}_0$ and follow its dynamical evolution. The inner and outer radii of the ring are assumed to be $R_{\mathrm{in}} = 5$ kpc and $R_{\mathrm{out}} = 7$ kpc, and its thickness to be 0.4 kpc at the initial stage. The outer radius of the disk is assumed to be $R = 7$ kpc. Particles are distributed randomly to reproduce uniform density. The initial velocity of each particle is taken in such a way that the centrifugal force is balanced by the gravitational force. Since the initial condition is not a steady state of the ring, the ring is soon deformed into a elongated shape perpendicular to the major axis of the potential and is relaxed into a quasi–steady state in which it takes time longer than the rotation period of the ring to change its shape. After then, the ring is gradually deformed. In model PB, as described in § III, we take another initial condition because of violent motion which occurred in the first stage of ring deformation. We put the ring in a rounder potential than the one adopted in model PB and pursue the motion of the ring in a few rotation periods. The ring deforms gradually in the initial deformation stage and attains the quasi–steady state. We adopt the ring in this stage as the initial condition for model PB and avoid an occurrence of violent motion in the first stage of ring deformation.

III. NUMERICAL RESULTS FOR A TUMBLING PROLATE POTENTIAL

In this section, we take three logarithmic models for the prolate potential with $a = 200$ pc and $b = c = 170$ pc; $a = 200$ pc and $b = c = 160$ pc; and $a = 200$ pc and $b = c = 150$ pc. The tumble axis of the potential is the Z-axis. As shown in Paper I, in the nontumbling prolate potential with $a = 200$ pc and $b = c = 150$ pc the gas ring precesses around the symmetry axis of the potential and finally settles into the equatorial plane of the potential within a few $\times\ 10^9$ yr due to differential precession and the dissipative property of gas.

In the tumbling prolate potential, the precession rate of the angular momentum vector of each gas particle is different from the nontumbling case. We briefly discuss the precession rate of the angular momentum vector of each gas particle. If we assume that the asphericity of the potential is small, and that ω_t is smaller than ω_0 and the precession rate in the nontumbling potential, ω_{p0}, which is the precession rate around the symmetry axis in the prolate potential and depends on a radius of particle orbit and an angle between the angular momentum vector and the symmetric axis of the potential, the precession rate of a circular closed orbit is given in the rotating frame of the tumbling prolate potential as

$$\omega_p = \frac{d\phi}{dt} = -\omega_0\left(\frac{3}{2}J_{20} - 3J_{22}\cos 2\phi\right)\cos\theta - \omega_t\,, \quad (3)$$

and

$$\Omega_p = \frac{d\theta}{dt} = \omega_0 3J_{22}\sin\theta\sin 2\phi\,, \quad (4)$$

where θ is the angle between the angular momentum vector of a gas particle and the Z-axis in the corotating frame of the potential, and ϕ is the angle between its projected angular momentum vector in the X-Y plane and the X-axis (Steiman-Cameron and Durisen 1984; Paper I). The aspherical parameters J_{20} and J_{22} are given as

$$J_{20} = \frac{1}{2}\frac{\varepsilon_1 + \varepsilon_2}{3 - \varepsilon_1 - \varepsilon_2}\,, \quad (5)$$

and

$$J_{22} = \frac{1}{4}\frac{\varepsilon_2 - \varepsilon_1}{3 - \varepsilon_1 - \varepsilon_2}\,, \quad (6)$$

where

$$\varepsilon_1 = \frac{a^2 - c^2}{a^2}\,, \quad \varepsilon_2 = \frac{b^2 - c^2}{b^2}\,.$$

Analytical solutions of equations (3) and (4), given by Steiman-Cameron and Durisen (1984) and Tohline and Durisen (1982), indicated that the precession trajectories are different in three regions. The precession trajectories of the angular momentum

TABLE 1

CALCULATED MODELS AND RESULTS FOR A PROLATE POTENTIAL

Model	a, b, c (pc)	ω_t (yr^{-1})	θ_i	t_p (yr)	L_f/L_0	θ_f	t_d (yr)	t_f (yr)
PA	200, 170, 170	$2\pi \times 10^{-9}$	10°	7.0×10^8	0.63	0°	...[a]	4.3×10^9
PB	200, 160, 160	$2\pi \times 10^{-9}$	10°	6.5×10^8	0.14	...[a]	...[a]	4.4×10^9
PC	200, 150, 150	$2\pi \times 10^{-9}$	0°[b]	...	0.28	...[a]	...[a]	7.4×10^8
PD	200, 150, 150	$2\pi \times 10^{-9}$	30°[b]	7.0×10^8	0.80	63°[b]	1.2×10^9	2.2×10^9

[a] The gas motion has not attained a steady state at time t_f.
[b] The angle between the angular mometum $\boldsymbol{L}$ and the minus Z-axis is given.

vectors of particles in circular orbits in the tumbling potential with $a = 200$ pc and $b = c = 160$ pc are shown in Figures 1*a* and 1*b* with $\omega_t = 0.01\omega_0$ and $\omega_t = 0.1\omega_0$, respectively. We call the region with $\omega_0 > \omega_{p0} \gg \omega_t$ region A (Fig. 1*a*). Region B (Fig. 1*b*) is defined for the case with $\omega_0 \gtrsim \omega_t \sim \omega_{p0}$, and region C is defined for the case with $\omega_t \gg \omega_0 > \omega_{p0}$. In region A, ω_t can be neglected in equation (3), and the precession trajectories are the same as in the nontumbling potential except for a tiny region around the positive Z-axis where there is a prograde preferred plane (Steiman-Cameron and Durisen 1984). Therefore, in region A the preferred planes are the same as in the non-tumbling potential except for the tiny region around the positive Z-axis. In region B, since ω_t is comparable with ω_{p0}, the precession trajectories are affected by the tumbling of the potential. As shown in Paper I, the central axis of the precession trajectories is normal to the neighboring preferred plane. Figure 1*b* indicates that two preferred planes are tilted from the symmetry axis of the potential in region B. Gas in these preferred planes rotates in the retrograde sense viewed from the rotation axis. The other preferred plane is normal to the tumbling axis of the potential for gas rotating in the prograde sense. In region C, since ω_t is very much larger than ω_0 and ω_{p0}, the time-averaged potential experienced by gas particles becomes essentially equal to the case with an axisymmetric potential in which the symmetry axis is the Z-axis. In this case, the preferred planes are the same as in the nontumbling potential with the Z-axis as the symmetry axis.

In the region B, there are the inner Lindblad resonance orbit, the corotation resonance orbit, and the outer Lindblad resonance orbit. Accordingly, we can expect that the gas motion is affected by the tumbling of the potential in region B. We calculate four models in region B, as shown in Table 1, in which we summarize the model parameters. We present the numerical results of our models below.

a) Prograde Case

In model PA, the gravitational potential with $a = 200$ pc and $b = c = 170$ pc is taken, and its tumbling rate is $\omega_t = 2\pi \times 10^{-9}$ yr^{-1}. The tumble axis is the shortest axis of this potential. The initial angular momentum vector of the gas ring tilts $\theta_i = 10°$ from the Z-axis in the X-Z plane. The gas ring rotates in a prograde sense. As shown in Figure 1, the precession trajectories of prograde orbits precess about the tumble axis. We calculate the motion of the gas ring for $t_f = 4.3 \times 10^9$ yr and find that the gas ring precesses as a whole with a period $t_p = 7.0 \times 10^8$ yr in the rotating frame, as indicated by arrows in Figure 1, and does not settle to any plane. At $t_f = 4.3 \times 10^9$ yr, the total angular momentum is $L_f = 0.63\,|\boldsymbol{L}_0|$, where $\boldsymbol{L}_0$ is the initial angular momentum of the gas ring. In the nontumbling case, the gas ring with the same initial condition settles into the plane perpendicular to the major axis within 4×10^9 yr, and its final angular momentum is $L_f = 0.19\,|\boldsymbol{L}_0|$ (Paper I). The final figure of the gas ring in Figure 2 is elongated in the direction perpendicular to the major axis.

In model PB, the adopted potential with $a = 200$ pc, $b = c = 160$ pc is more elongated than that in model PA. The tumbling rate is $\omega_t = 2\pi \times 10^{-9}$ yr^{-1}, and the initial angular momentum vector of the gas ring is tilted $\theta_i = 10°$ from the Z-axis in the X-Z plane. Since the gas ring is soon highly deformed and elongated perpendicularly to the major axis, shock waves occur in the gas ring, and about two-thirds of its angular momentum is dissipated within $t = 2 \times 10^8$ yr. Finally, the gas concentrates into the center of the potential. Since the gas ring with this initial condition is disrupted soon, we adopted another initial condition as follows. We put the gas ring in the prolate potential with $a = 200$ pc, and $b = c = 180$ pc with same tumbling rate, pursue the time evolution for four rotation periods, and obtain a deformed ring in the quasi–steady state. We adopt the gas ring in this stage as the initial condition for model PB where $b = c = 160$ pc. In this case, as shown in Figure 3, the gas ring is deformed rather gradually. We calculate the motion of the gas ring for $t_f = 4.4 \times 10^9$ yr, and find the gas ring precesses as a whole and does not settle to any plane as does model PA. Some part of the gas ring concentrates in the central region. The results of models PA and PB suggest that in the plane perpendicular to the tumbling axis, which is the shortest axis of the prolate potential, it takes a long time for the gas with prograde rotation to settle into the preferred plane as compared with the nontumbling case, if it settles into the preferred plane.

b) Retrograde Case

In model PC, the potential with $a = 200$ pc and $b = c = 150$ pc is taken with $\omega_t = 2\pi \times 10^{-9}$ yr^{-1}. The initial angular momentum vector of the gas ring is directed along the minus Z-axis. That is, the initial gas ring rotates in a retrograde sense. At first, the vertical random motion of gas particles in the ring becomes large, the angular momentum of the gas ring decreases, and finally almost all the gas concentrates into the center of the potential within 10^9 yr, as shown in Figure 4. The mechanism of the decrease of angular momentum is as follows: as seen in Figure 1*b*, the precession trajectories cross each other at the minus Z-axis in region B. The direction of the angular momentum vector of individual gas particles fluctuates due to the random motion of gas particles and precesses in the direction of arrows shown in Figure 1. As time goes on, the difference of angular momentum vectors increases. Finally the gas collides supersonically, a shock wave occurs, and the difference of the angular momenta is dissipated. This behavior of the gas motion is similar to model TC in Paper I, in which the

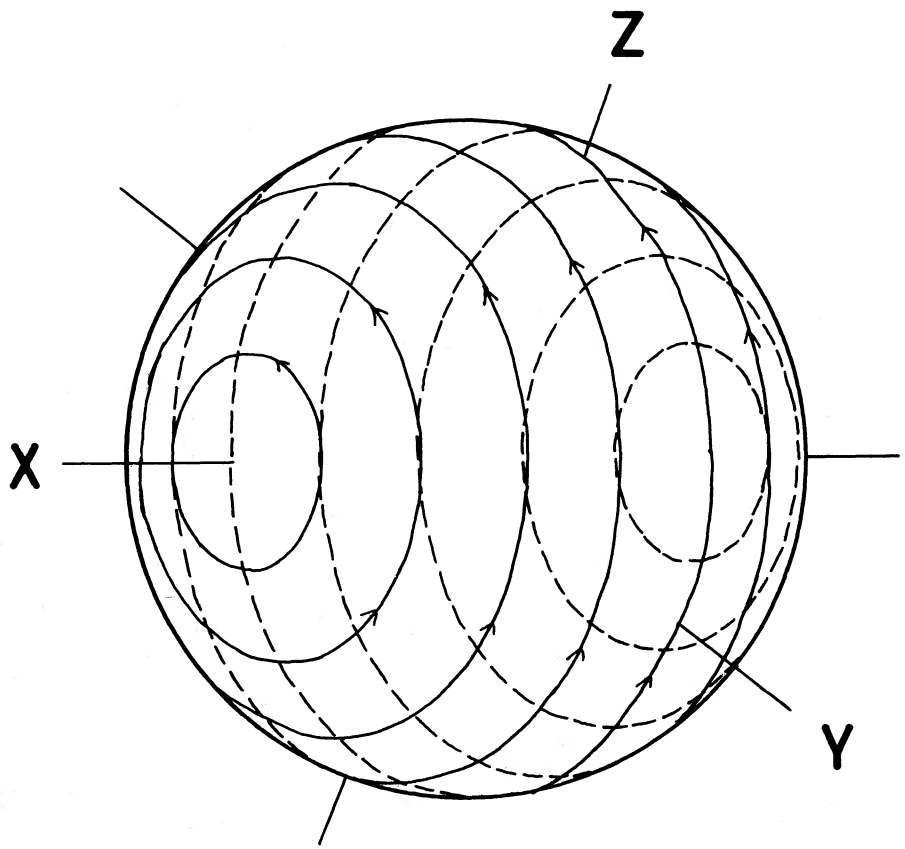

FIG. 1a

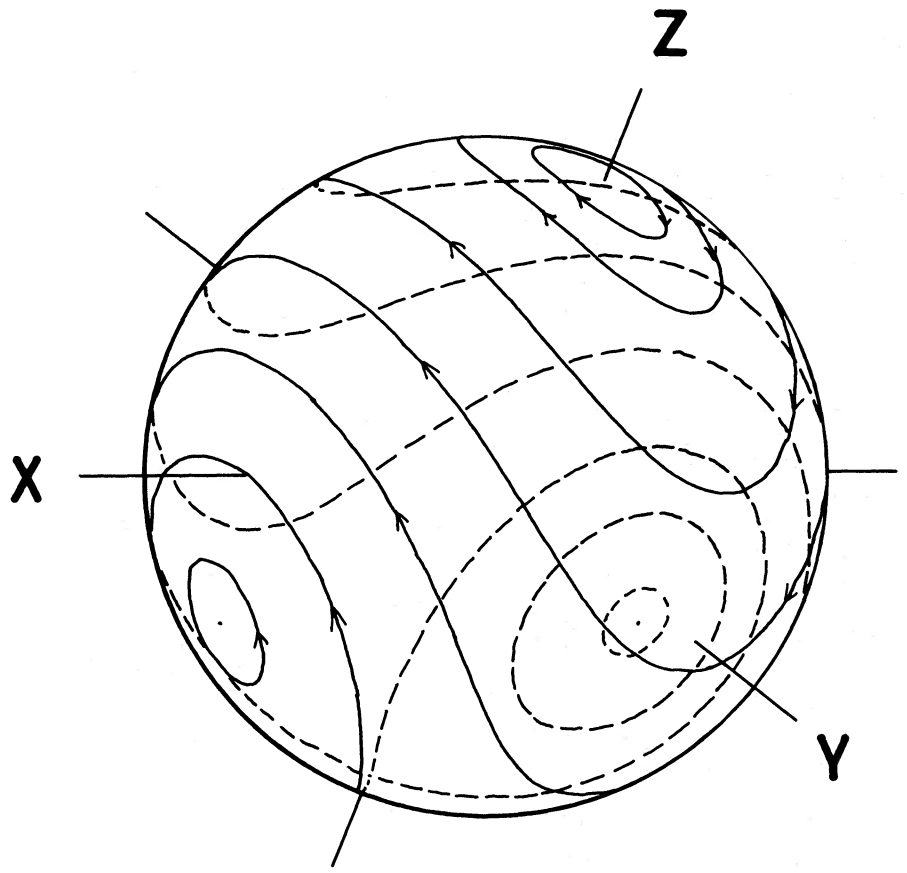

FIG. 1b

FIG. 1.—Precession trajectories of the angular momentum vector of a single particle circular orbit in the corotating frame of the tumbling prolate potential with $a = 200$ pc and $b = c = 160$ pc. The tumbling axis is the Z-axis. Trajectories in (*a*) region A with $\omega_t = 0.01\omega_0$, and (*b*) region B with $\omega_t = 0.1\omega_0$. Solid lines show the precession trajectories on the near side, and dashed lines do on the far side.

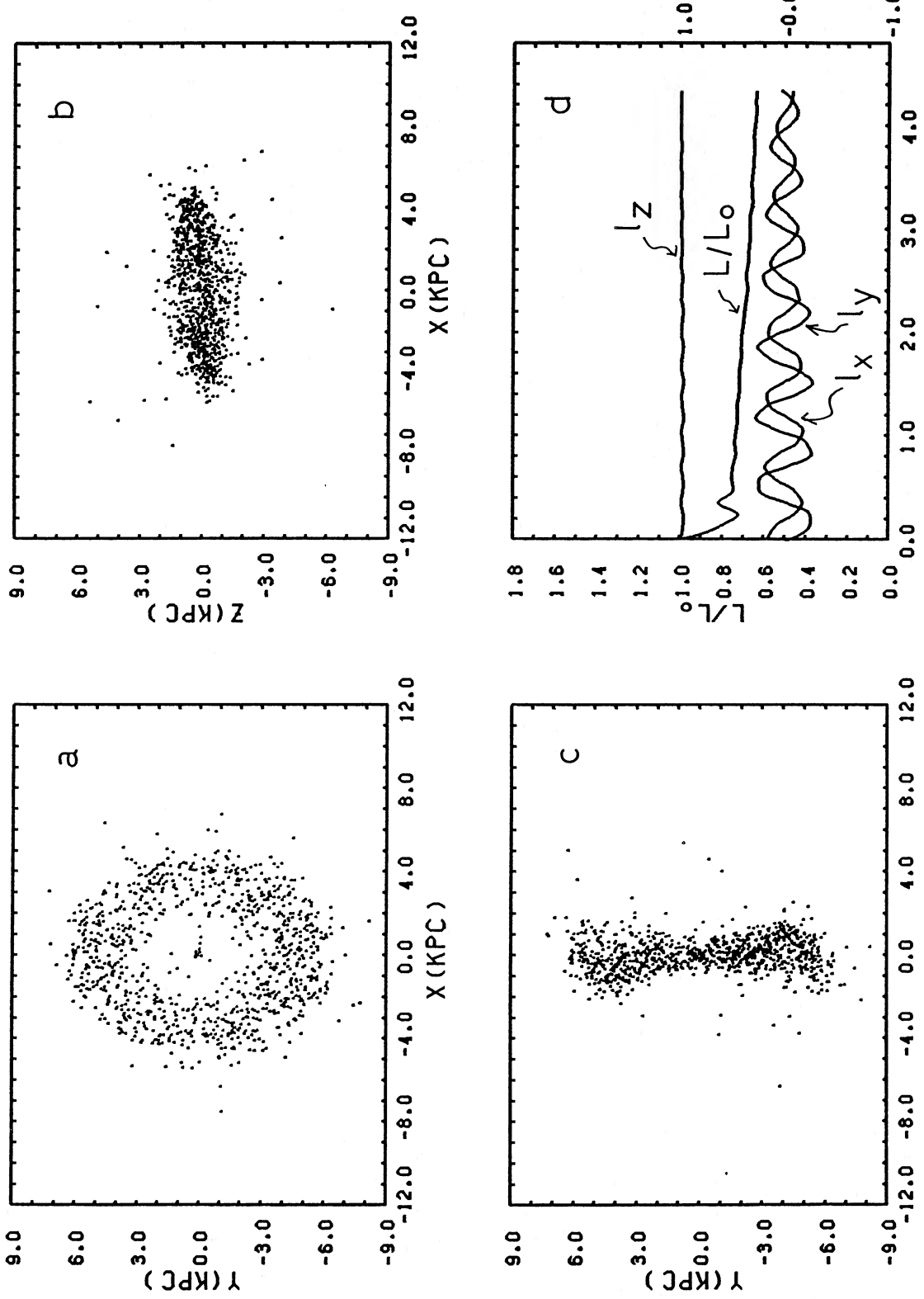

FIG. 2.—Projected distributions of gas particles for model PA at $t = 4.3 \times 10^9$ yr. Projections of gas particles onto (*a*) the *X*-*Y* plane, (*b*) the *X*-*Z* plane, and (*c*) the *Z*-*Y* plane, in the corotating frame. (*d*) Time variations of the total angular momentum of the gas ring $|L|/L_0$ (*scale on the left*) and of each component in the corotating frame as $l_i = L_i/|L|(i = X, Y, Z)$ (*scale on the right*). The gas ring precesses as a whole and has not settled into any preferred plane as yet.

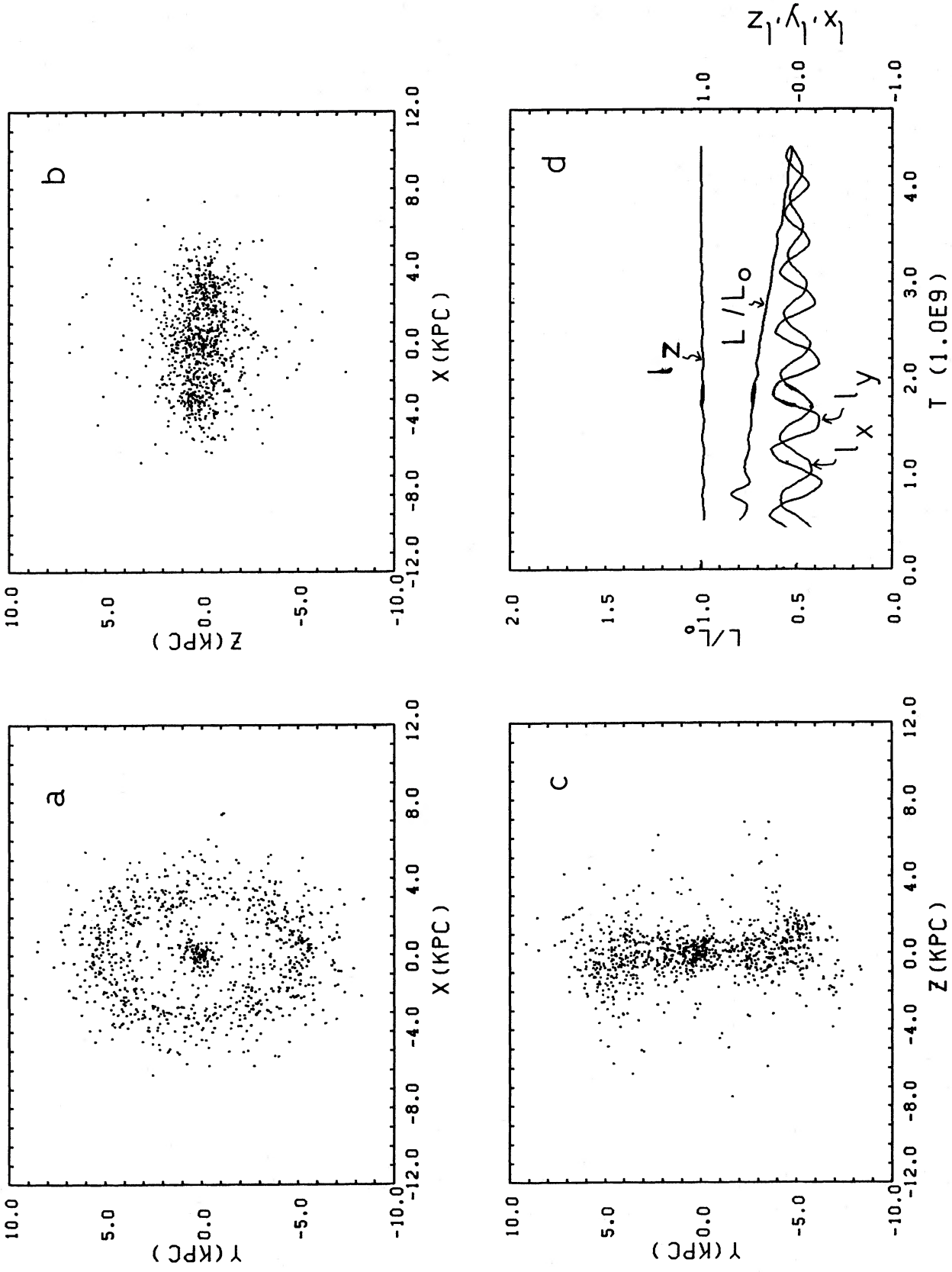

FIG. 3.—Same as Fig. 2, but for model PB at $t = 4.4 \times 10^9$ yr. Some gas concentrates near the center.

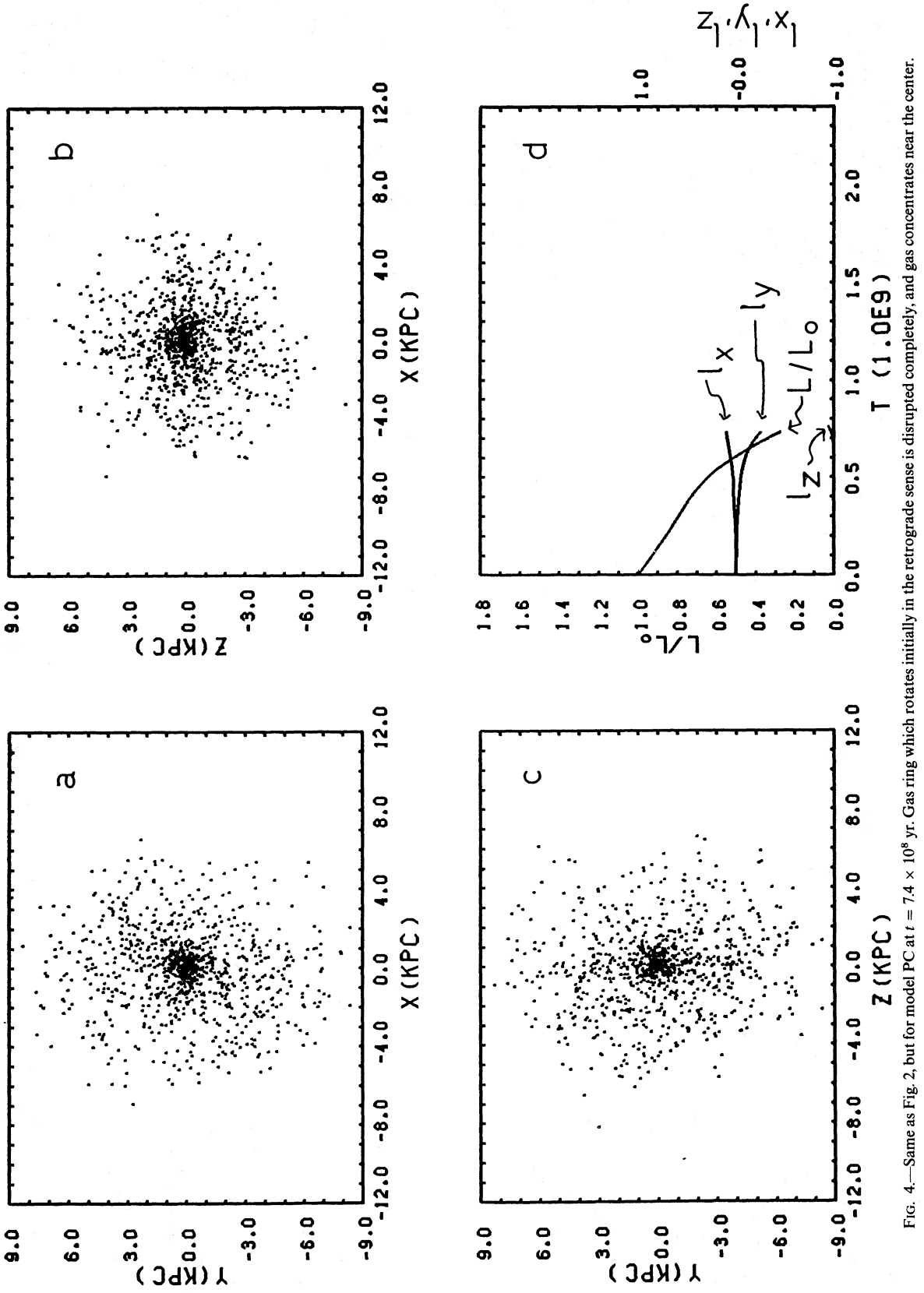

FIG. 4.—Same as Fig. 2, but for model PC at $t = 7.4 \times 10^8$ yr. Gas ring which rotates initially in the retrograde sense is disrupted completely, and gas concentrates near the center.

TABLE 2

CALCULATED MODELS AND RESULTS FOR A TRIAXIAL POTENTIAL

Model	a, b, c (pc)	ω_t (yr^{-1})	θ_i	t_p (yr)	L_f/L_0	θ_f	t_d (yr)	t_f (yr)
TA	200, 180, 150	$2\pi \times 10^{-9}$	10°	3.8×10^8	0.88	0°	1.7×10^9	2.4×10^9
TB	200, 180, 150	$4\pi \times 10^{-8}$	30°	0.5×10^8	0.82	0°	...[a]	3.3×10^9
TC	200, 180, 150	$2\pi \times 10^{-9}$	10°[b]	1.1×10^9	0.90	0°[b]	1.2×10^9	2.2×10^9
TD	200, 160, 150	$2\pi \times 10^{-9}$	0°[b]	...	0.30	...	...[a]	1.6×10^9
TE	200, 180, 150	$4\pi \times 10^{-9}$	0°[b]	...	0.94	0°[b]	...[a]	2.4×10^9
TF	200, 160, 150	$4\pi \times 10^{-9}$	30°[b]	8.0×10^8	0.78	55°[b]	0.8×10^9	1.3×10^9
TG	200, 180, 150	$4\pi \times 10^{-9}$	30°[b]	1.0×10^9	0.64	57°[b]	1.6×10^9	2.0×10^9

[a] The gas motion has not attained a steady state at time t_f.
[b] The angle between the angular momentum $\boldsymbol{L}$ and the minus Z-axis is given.

initial angular momentum vector of the gas ring is directed along the intermediate axis of a triaxial potential. We also calculated a rounder potential case than model PC for comparison, i.e., a prolate potential with $a = 200$ pc and $b = c = 180$ pc. Although the vertical random motion of gas particles in the ring becomes large, it is not large enough to induce shock waves within 10^9 yr. Therefore, much more time is necessary for gas to concentrate to the center of the potential.

c) *Anomalous Case*

The model PD is the same potential as model PC, except that the initial gas is distributed uniformly in a disk with a radius 8 kpc and a thickness 400 pc. We set the initial angular momentum vector of the gas disk tilted 30° from the minus Z-axis in the X-Z plane. The gas disk rotates in a retrograde sense as viewed looking down the tumble axis. As shown in Figure 5, the angular momentum vector of the gas disk precesses around the anomalous preferred plane and after $t = 1.2 \times 10^9$ yr the angular momentum vector of the gas disk settles into the X-Z plane. The final gas disk is warped. The final angular momentum L_f is $L_f/|\boldsymbol{L}_0| = 0.8$, and its component ratio is $L_x : L_y : L_z = 0.89 : 0.0 : 0.45$, where $\boldsymbol{L}_0$ is the initial angular momentum. Since every part of the gas disk has the same precession rate and this precession rate is equal to the tumble rate of the potential, the final warped gas disk is steady. van Alvada, Kotanyi, and Schwarzschild (1982) and Steiman-Cameron and Durisen (1984) have found the analytic solution of this type in the case of a slightly deformed potential, and Heisler, Merritt, and Schwarzschild (1982) and Magnenant (1982) have presented the stable particle orbits of this type for a triaxial potential. Here we have clearly shown that the gas settles into the preferred plane of this type by numerical calculations.

IV. NUMERICAL RESULTS FOR A TUMBLING TRIAXIAL POTENTIAL

We first show the precession trajectories for a tumbling triaxial potential to see the effect of potential tumbling on the gas motion. The equations for precession trajectories in a tumbling potential are the same as in equations (3) and (4). Figure 6 shows the trajectories in a tumbling potential with $a = 200$ pc, $b = 180$ pc, and $c = 150$ pc, with $\omega_t = 2\pi \times 10^{-9}$ yr^{-1}. The precession trajectories are different in three regions, the same as in the case of the tumbling prolate potential. We also name region A as the region with $\omega_0 > \omega_{p0} \gg \omega_t$, region B as $\omega_0 \gtrsim \omega_t \sim \omega_{p0}$, and region C as $\omega_t \gg \omega_0 > \omega_{p0}$. Since ω_t can be neglected in equation (3) in region A, the preferred planes in region A are the same as in the nontumbling potential case. Since ω_t is much larger than ω_0 and ω_{p0} in region C, the gravitational force on the gas can be averaged over the time $2\pi/\omega_t$, and the precession trajectories are the same as in an axisymmetric potential. In region B, the precession trajectories are strongly affected by the potential tumbling as shown in Figure 6. From the precession trajectories, we can expect the presence of four stable orbits, which are the prograde orbit in the plane normal to the tumble axis, the retrograde orbit in the plane normal to the tumble axis, and two retrograde orbits tilted with respect to the tumble axis.

Mulder (1983) stressed finding stable prograde orbits at $r \sim 2r$ (corotation radius) tilted with respect to the tumble axis. These stable orbits are not indicated from the study of precession trajectories. We examine by numerical calculations whether Mulder's stable orbits are preferred planes for gas or not.

We summarize our numerical results in Table 2. We take two logarithmic models for triaxial potentials with either $a = 200$ pc, $b = 180$ pc, and $c = 150$ pc or $a = 200$ pc, $b = 160$ pc, and $c = 150$ pc. The tumble axis is the shortest (Z) axis of the potential, and the tumbling rate ω_t is taken $2\pi \times 10^{-9}$ yr^{-1}, $4\pi \times 10^{-9}$ yr^{-1}, or $4\pi \times 10^{-8}$ yr^{-1}.

a) *Prograde Gas Ring*

We show first the numerical results for a gas ring rotating in the prograde sense. In model TA, we take the triaxial potential with $a = 200$ pc, $b = 180$ pc, and $c = 150$ pc and the tumbling rate as $\omega_t = 2\pi \times 10^{-9}$ yr^{-1}. The angular momentum vector of the gas ring is initially tilted $\theta_i = 10°$ from the Z-axis in the X-Z plane. With the angular momentum vector of the ring precessing around the Z-axis differentially, the component of the angular momentum vector perpendicular to the tumble axis is gradually lost due to a shock wave caused by the collision of gas flow. Finally, the gas settles into the X-Y plane after $t_d = 2 \times 10^9$ yr as shown in Figure 7. In order to see whether or not the preferred plane consists of Mulder's stable prograde orbits, we calculate model TB. In model TB, we take the potential with $a = 200$ pc, $b = 180$ pc, and $c = 150$ pc and the tumbling rate $\omega_t = 4\pi \times 10^{-8}$ yr^{-1}. The initial gas ring with $r_{in} = 4$ kpc and $r_{out} = 7$ kpc is tilted $\theta_i = 30°$ from the Z-axis in the X-Z plane and rotates in a prograde sense. The corotation radius is 2.5 kpc, and the radius of the outer Lindblad resonance is 5 kpc. Any preferred plane tilted from the Z-axis is expected to consist of the Mulder's stable prograde orbits between the radii of corotation and the outer Lindblad resonance. After $t = 3.3 \times 10^9$ yr as shown in Figure 8, although the component of the angular momentum vector normal to the Z-axis decreases due to the differential precession, the gas does

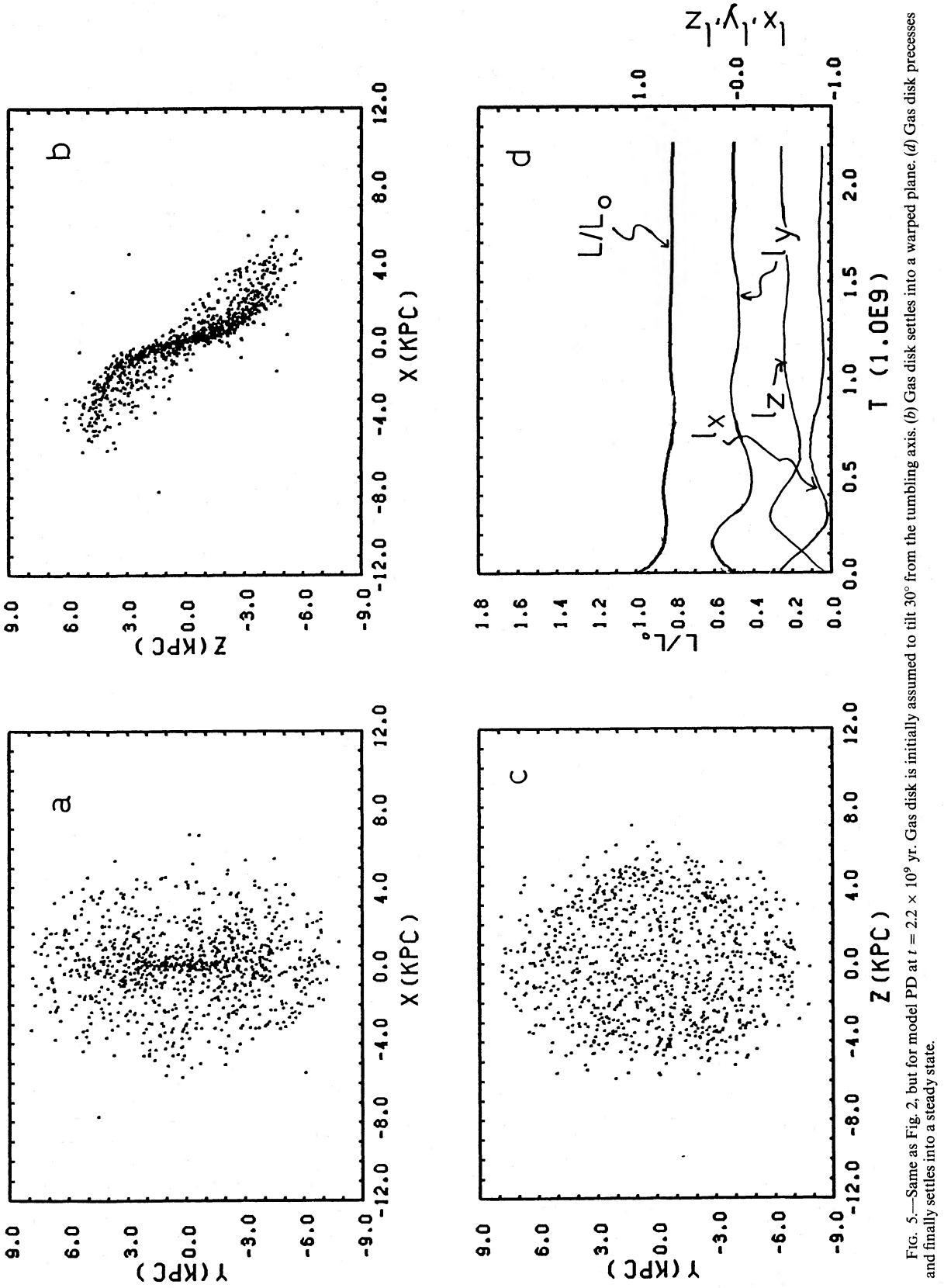

FIG. 5.—Same as Fig. 2, but for model PD at $t = 2.2 \times 10^9$ yr. Gas disk is initially assumed to tilt 30° from the tumbling axis. (*b*) Gas disk settles into a warped plane. (*d*) Gas disk precesses and finally settles into a steady state.

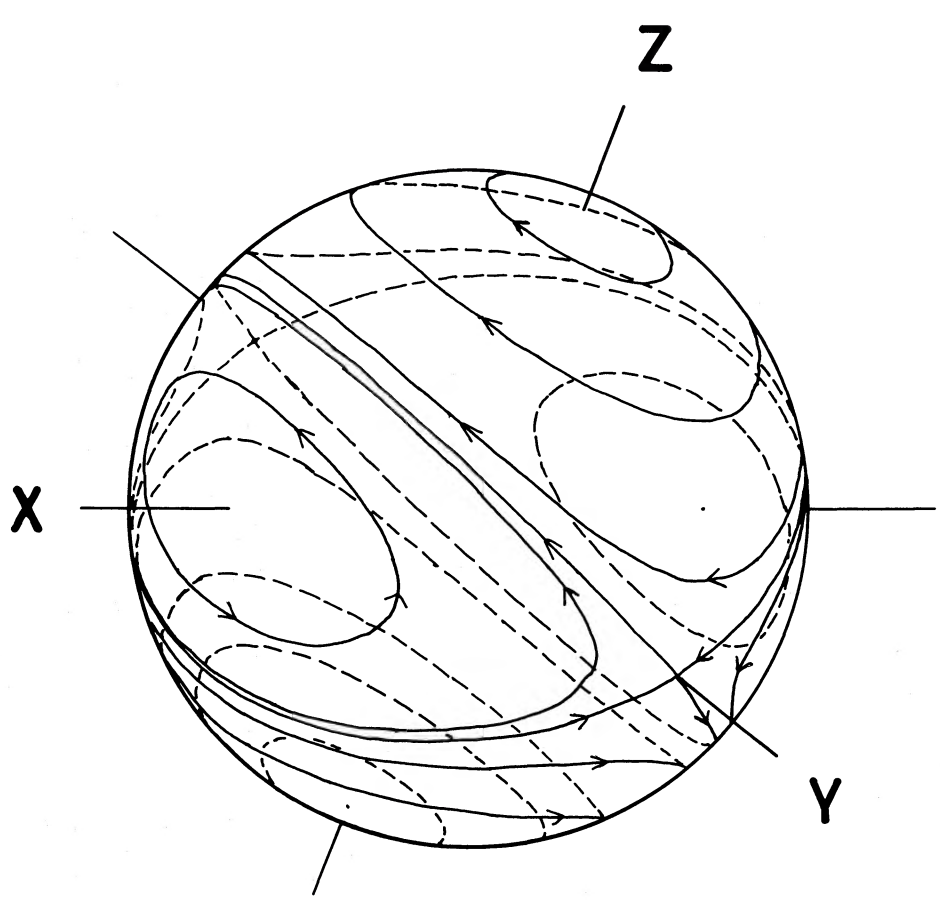

FIG. 6a

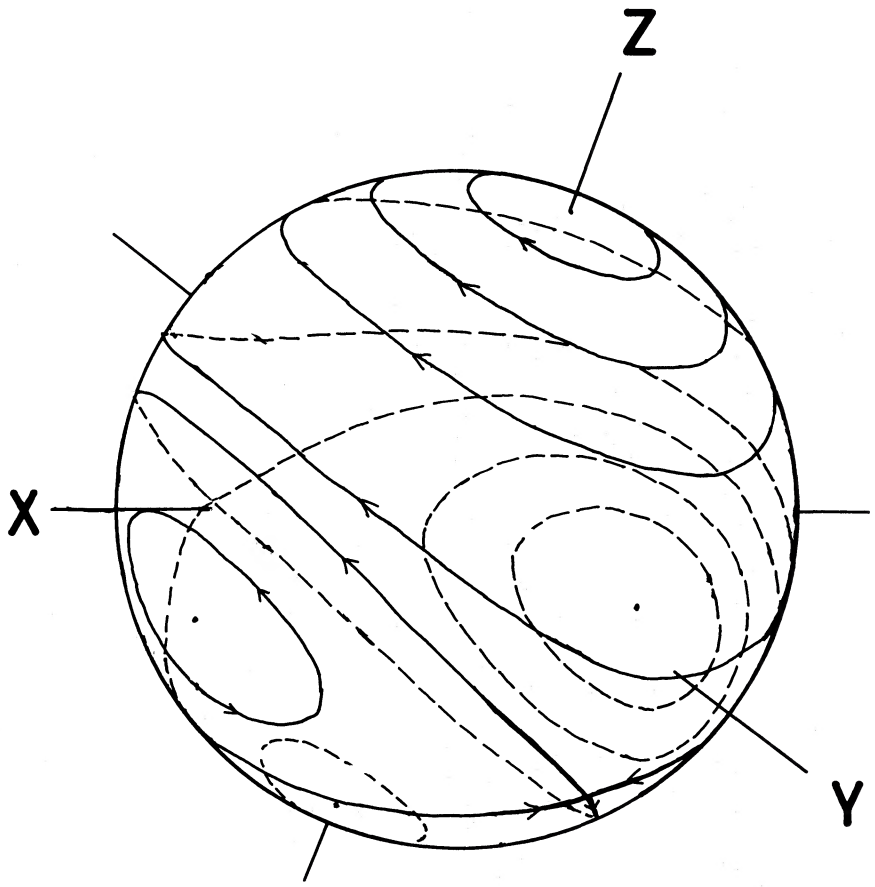

FIG. 6b

FIG. 6.—Same as Fig. 1, but for the tumble triaxial potential with $a = 200$ pc, $b = 180$ pc, and $c = 150$ pc. Tumble axis is the Z-axis. Precession trajectories in (*a*) region A and (*b*) region B.

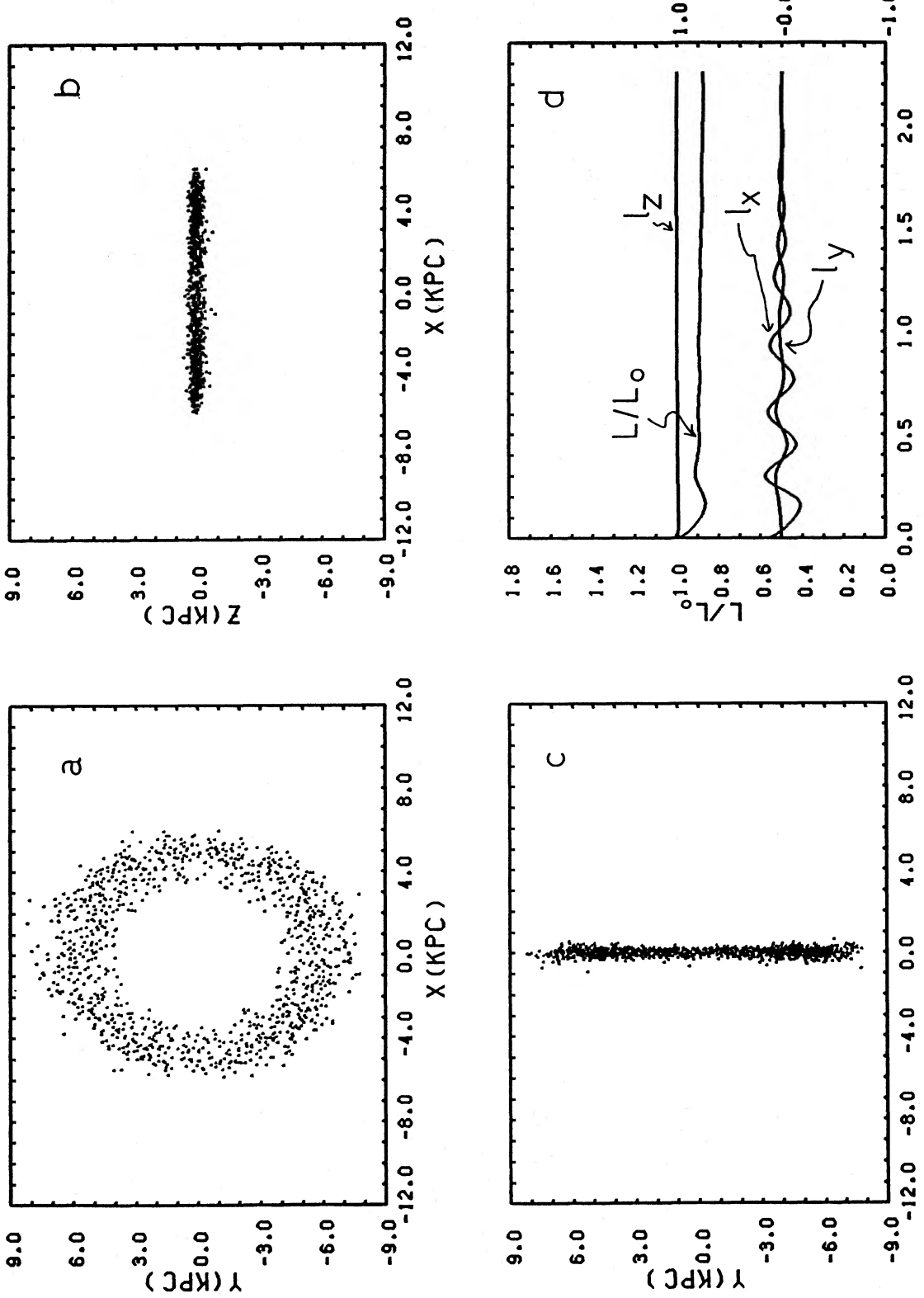

FIG. 7.—Same as Fig. 2, but for model TA at $t = 2.4 \times 10^9$ yr. Triaxial potential tumbles at $\omega_t = 2\pi \times 10^{-9}$ yr^{-1}. The initial gas ring tilted 10° from the Z-axis in the X-Z plane with prograde rotation finally settles into the plane perpendicular to the tumbling axis.

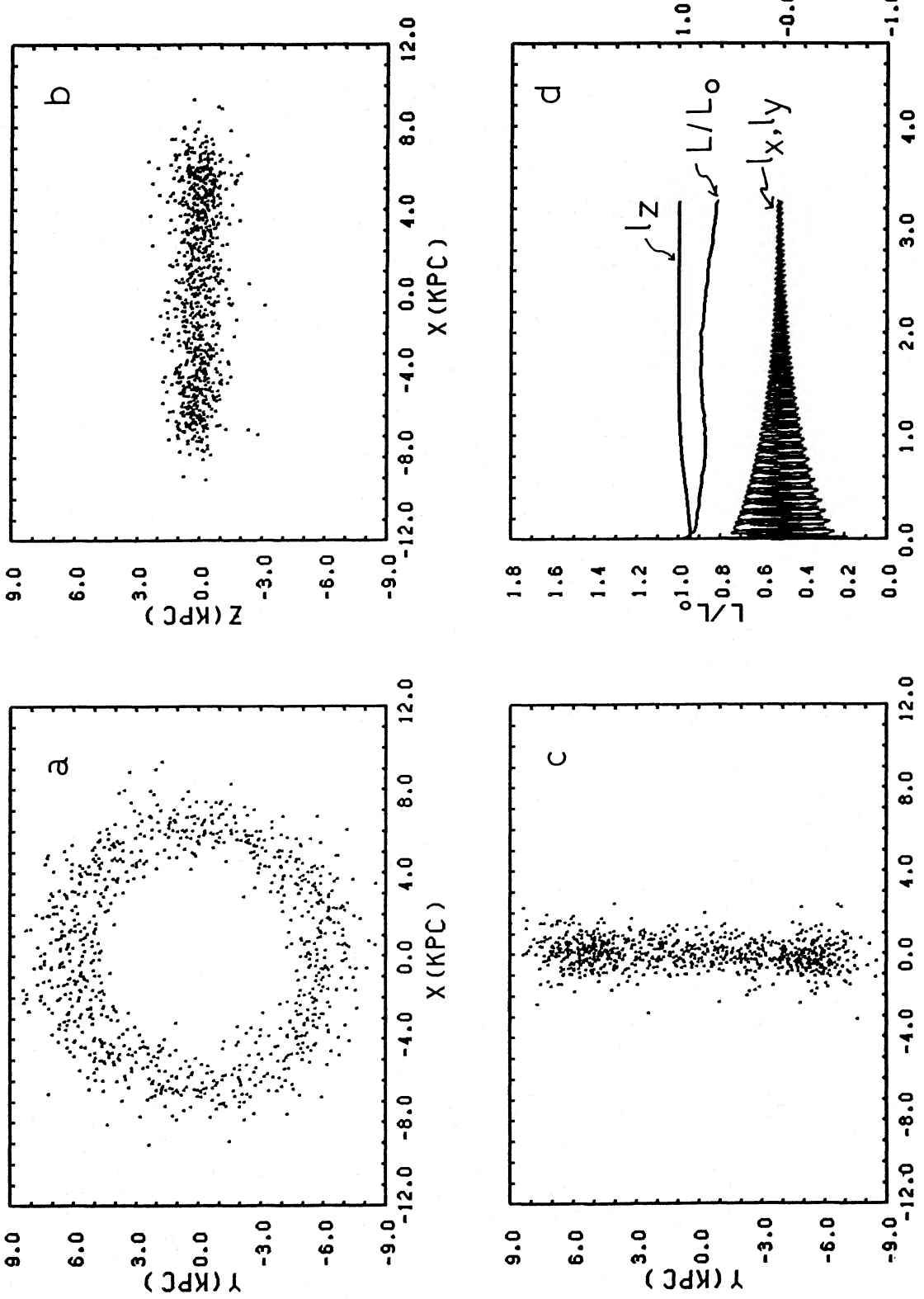

FIG. 8.—Same as Fig. 2, but for model TB at $t = 3.3 \times 10^9$ yr. Triaxial potential tumbles at $\omega_t = 4\pi \times 10^{-8}$ yr^{-1}. Gas ring rotates initially in the prograde sense. The random motion of gas particles is excited and gas does not settle well.

not settle into any definite tilted planes. In model TA, the time needed to settle into the X-Y plane is 1.7×10^9 yr. In model TB, we follow the gas motion 3 times longer than in model TA, but the gas does not show any tendency to settle into tilted stable orbits. As shown by Binney (1978, 1981), gas motion parallel to the tumble (Z) axis can be excited by an orbit instability. Our result may indicate that Mulder's stable orbits are not preferred planes for dissipative gas particles. Other possibilities are that the time needed to settle into the Mulder's stable orbits is very long or the conditions needed to settle into the Mulder's stable orbits are very restrictive.

b) *Retrograde Gas Case*

In model TC, we take the triaxial potential with $a = 200$ pc, $b = 180$ pc, and $c = 150$ pc and the tumbling rate $\omega_t = 2\pi \times 10^{-9}$ yr^{-1}. The angular momentum vector of the gas disk is initially tilted 10° from the minus Z-axis in the X-Z plane and rotates in a retrograde sense. After $t_d = 10^9$ yr, the gas settles into the plane normal to the Z-axis. Before this stage, the component of angular momentum normal to the Z-axis has been lost, so that the total angular momentum decreases and a dense disk is formed in the central region. This disk corresponds to a preferred plane in the present case. This result is consistent with the precession trajectories in this potential for the tumbling rate specified above. But in the case of a higher tumbling rate or a more elongated potential, the plane normal to the Z-axis cannot be a preferred plane. Model TD is one example of the more elongated potential case.

In model TD, we take the triaxial potential with $a = 200$ pc, $b = 160$ pc, and $c = 150$ pc and the tumbling rate $\omega_t = 2\pi \times 10^{-9}$ yr^{-1}. The initial gas ring is set in the plane normal to the Z-axis and rotates in a retrograde sense. As shown in Figure 9, after $t = 1.6 \times 10^9$ yr, the total angular momentum decreases to $L = 0.3|\boldsymbol{L}_0|$ and the gas concentrates into the center. This result is consistent with the precession trajectories of retrograde orbits which cross each other at the Z-axis in model TD.

Model TE is the same as model TD, except we use the triaxial potential with $a = 200$ pc, $b = 180$ pc, and $c = 150$ pc and the tumbling rate $\omega_t = 4\pi \times 10^{-9}$ yr^{-1}. After 2×10^9 yr, the random motion of gas increases gradually, since the precession trajectories cross each other at the Z-axis, even though not so violently. This result indicates that much time is needed for a gas ring to be disrupted in a relatively round potential.

In model TF, we take the triaxial potential with $a = 200$ pc, $b = 160$ pc, and $c = 150$ pc and the tumbling rate $\omega_t = 4\pi \times 10^{-9}$ yr^{-1}. The initial gas disk has the radius $r = 8$ kpc, and its angular momentum vector is tilted $\theta_i = 30°$ from the minus Z-axis in the X-Z plane. The gas disk precesses differentially, and after $t_d = 8.0 \times 10^8$ yr the gas disk attains a steady state in a rotating frame and precesses as a whole with the precession rate equal to the tumbling rate of the potential. As shown in Figure 10, the angle between the normal direction of the gas disk and the Z-axis is 50° within 5 kpc and becomes smaller at radii larger than 5 kpc. The gas disk is flat within 5 kpc. The warped gas disk formed outside 5 kpc is similar to the anomalous orbit shown in Figure 5.

In model TG, we take the triaxial potential with $a = 200$ pc, $b = 180$ pc, and $c = 150$ pc and the tumbling rate $\omega_t = 4\pi \times 10^{-9}$ yr^{-1}. The model TG is the same as model TF, including the initial conditions, except that it has a less elongated potential. The initial gas disk rotates in the retrograde sense. After 10^9 yr, the gas disk becomes warped and precesses as a whole with the precession rate equal to the tumbling rate of potential. The thickness of the gas disk is as large as 2 kpc, since the gas disk is not well settled yet. The gas settling time to this preferred plane in model TG is larger than that in model TF. The more elongated the triaxial potential is, the faster the gas settling is, and the steeper the angular momentum vector of the disk declines from the tumbling axis with increasing radius. The reason for this result is discussed in § V.

V. THE TIME SCALE FOR GAS SETTLING INTO THE WARPED PREFERRED PLANE

As shown in §§ III and IV, rotating gas in a tumbling prolate or triaxial potential settles into a preferred plane within the order of 10^9 yr, except for models PA, PB, and TB. The anomalous preferred planes are warped, while the preferred planes normal to the tumble axis are flat. In this section, we discuss the time scale for gas settling into the warped preferred plane and the relation of the shape of a warped preferred plane with the potential shape and its tumbling rate, except for models PA, PB, and TB.

Since the gas particles precess differentially and their orbits deform from circular orbits, the gas particles in different orbits can collide with each other, and the component of angular momentum normal to the precession axis dissipates by a shock wave. Finally the gas settles into the preferred plane. The time for the dissipation of angular momentum will be the order of the time it takes orbits of neighboring gas elements to precess differentially by a significant amount. This time is estimated as

$$t_d \sim \beta(\pi/2)/\Delta\omega_p , \tag{7}$$

where $\Delta\omega_p$ is the differential precession rate caused by the difference of the angular momentum vector of each gas particle due to random motion and β is a factor of order unity. For example, $\Delta\omega_p$ is

$$\Delta\omega_p = \omega_0\left(\frac{3}{2}J_{20} - 4J_{22}\right)(\sin\theta)(\Delta\theta) + \omega_0\left(\frac{3}{2}J_{20} - 3J_{22}\right)\cos\theta\,\frac{\Delta r}{r}, \tag{8}$$

where Δr is the difference of the orbit radius of gas ring particles which can collide with each other, and we assume the angle of angular momentum vector $\phi = 0$ and $\Delta\phi = 0$ for simplicity. If the random velocity of the gas is 10 km s^{-1} and the radius of a gas ring is 5 kpc, $\Delta\theta$ and $\Delta r/r$ are estimated as $\Delta\theta \sim \Delta r/r \sim 0.08$ (Paper I). For the logarithmic triaxial potential with $a = 200$ pc, $b = 180$ pc, and $c = 150$ pc, we have $\varepsilon_1 = 0.44$, $\varepsilon_2 = 0.31$, $J_{20} = 0.16$, and $J_{22} = -0.015$ from equation (5), and $\Delta\omega_p \sim 0.023\omega_0$ and $t_d \sim (11.0)(\beta)(2\pi/\omega_0)$ for $\theta = 10°$. From the comparison with the numerical results of this paper, β is as large as unity for the warped preferred plane, except for models PA, PB, and TB. In these models, the rotation of the gas ring is prograde. In model TB, since the orbital instability explored by Binney (1978, 1981) excites the gas motion perpendicular to the plane, the dissipation time is lengthened. Lengthening of the dissipation time in model PA and PB occurs, and these results agree with the analytic analyses of precession trajectories by Durisen *et al.* (1983). Equations (40) and (42) in their paper show that the rate of differential precession and hence of settling into the preferred plane perpendicular to the tumbling axis in a prolate potential is much slower than the tilted preferred planes. It should be noticed that, for the warped preferred plane, the tumbling rate

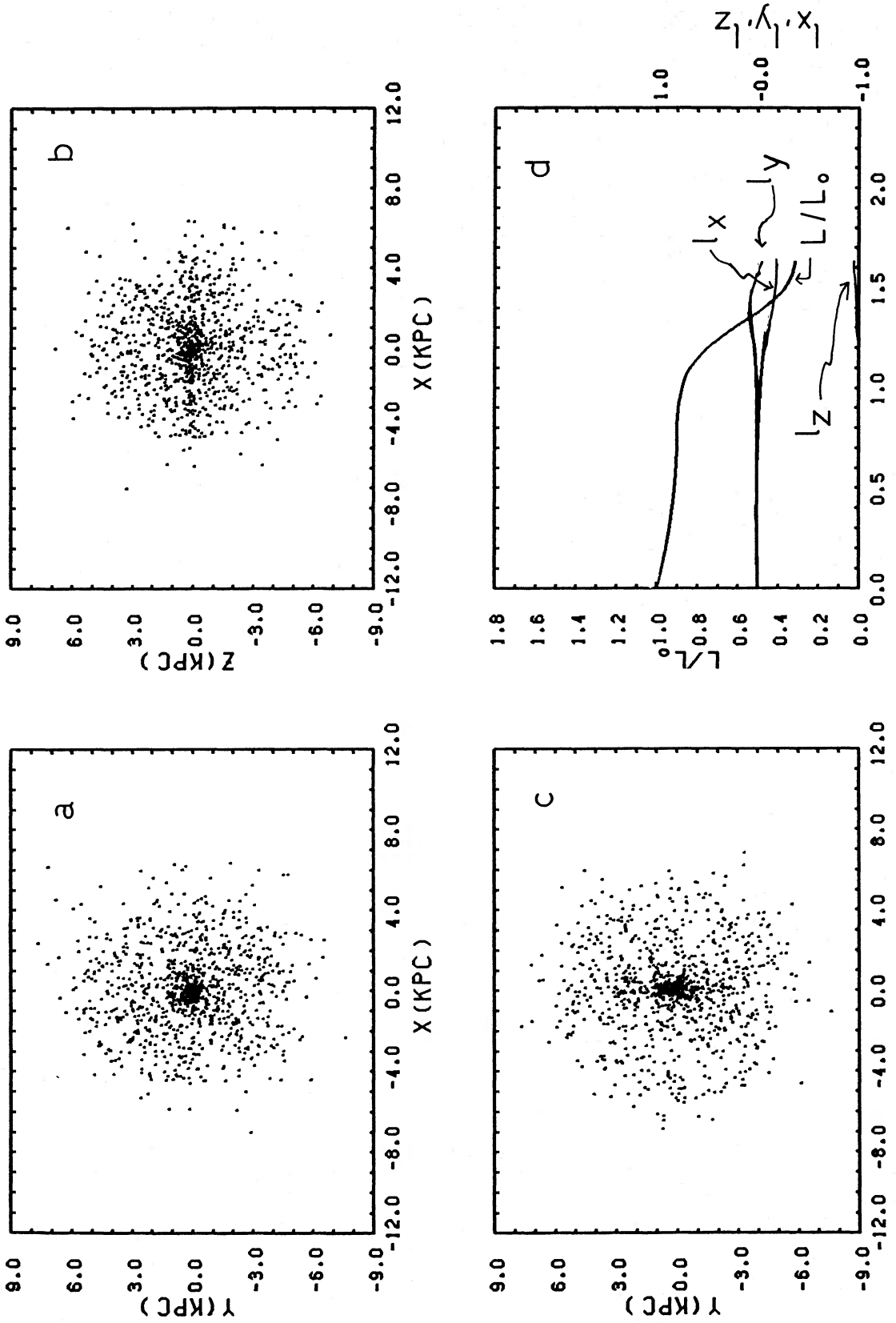

FIG. 9.—Same as Fig. 2, but for model TD at $t = 1.6 \times 10^9$ yr. Gas ring is disrupted completely, and gas concentrates near the center.

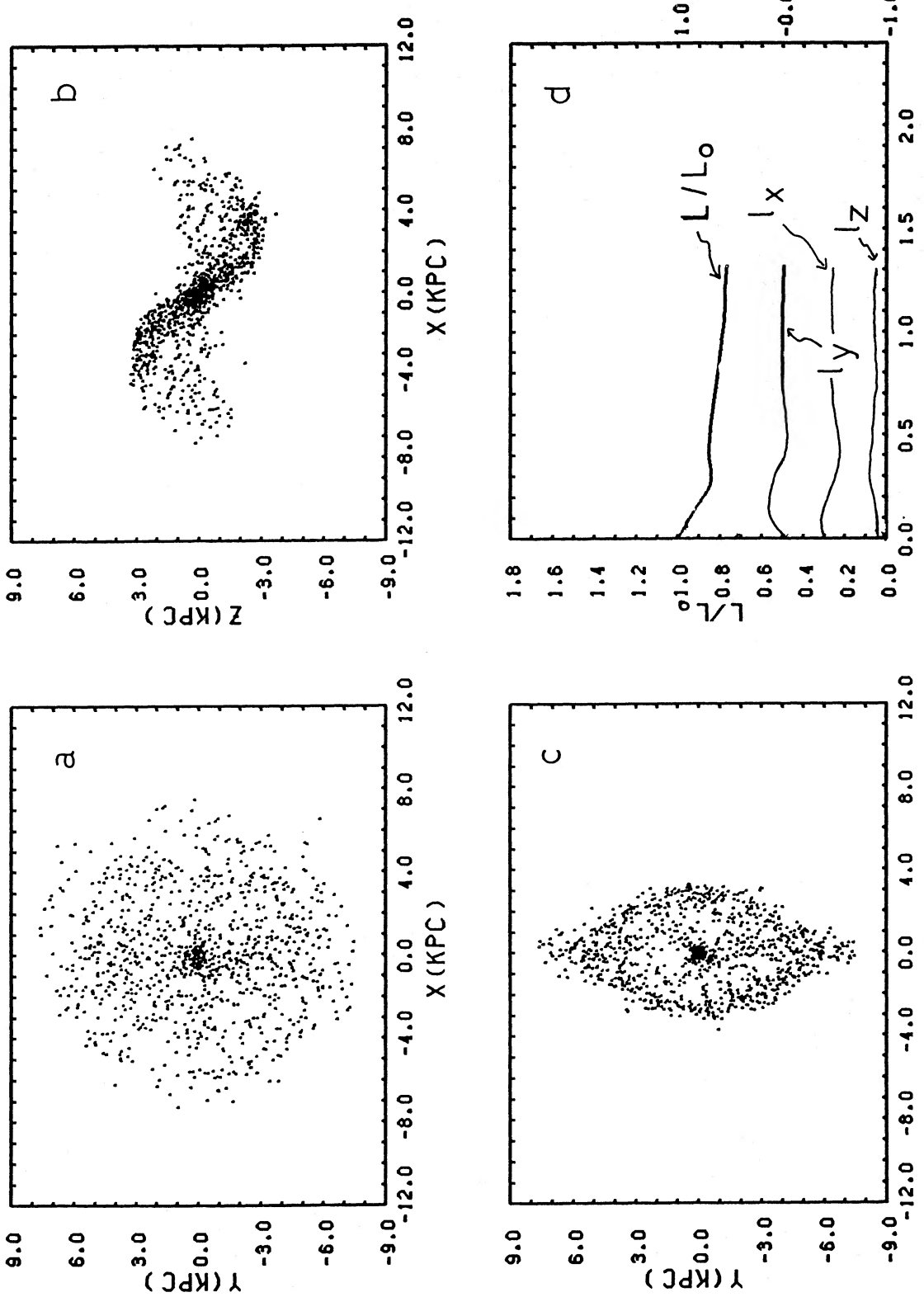

FIG. 10.—Same as Fig. 2, but for model TF at $t = 1.3 \times 10^9$ yr. Projections of gas particles onto (*a*) the *X*-*Y* plane, (*b*) the *X*-*Z* plane, and (*c*) the *Z*-*Y* plane, in the corotating frame. Gas disk settles into the warped plane. (*d*) Gas disk is steady as seen in (*d*).

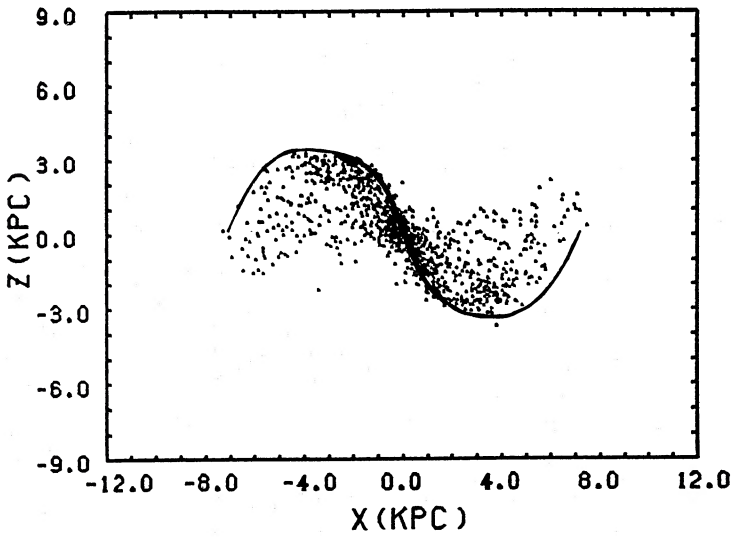

FIG. 11.—Approximate solution for the preferred plane in eq. (11) and the numerical results of model TF. These two results agree well.

ω_t does not affect the dissipation time as long as it is smaller than ω_0.

Next we show the relation of the shape of the warped preferred plane with the parameters of the tumbling potential. The shape of a warped preferred plane is determined by the condition that the tilted circular orbits do not precess in the rotating frame of the tumbling potential. This condition is expressed by $d\phi/dt = 0$ and $d\theta/dt = 0$ for each radius at which the preferred plane exists. From equations (3) and (4), we can obtain this condition as

$$-\omega_0(\tfrac{3}{2}J_{20} - 3J_{22}\cos 2\phi)\cos\theta - \omega_t = 0\,, \tag{9}$$

and

$$\omega_0 3J_{22}\sin\theta\sin 2\phi = 0\,. \tag{10}$$

If $\phi = 0$, equation (10) is automatically satisfied, and equation (9) leads to

$$\cos\theta = -\frac{\omega_t}{\omega_0}\frac{1}{(3/2)J_{20} - 3J_{22}}\,. \tag{11}$$

The solution in equation (11) for the warped preferred plane is given for a general tumbling triaxial potential in Table 1 of David, Steiman-Cameron, and Durisen (1985). Since ω_0, J_{20}, and J_{22} depend on r in general, the angle θ which satisfies equation (11) also depends on r. This implies that the preferred plane warps. If the absolute value of the right-hand side of equation (11) is greater than unity, the tilted preferred plane cannot exist. Although $\phi = \pi/2$ is another solution of equation (10), this corresponds to the unstable case. This is seen from the precession trajectories.

If the potential of a galaxy has the same form as in equation (1), we obtain $\omega_0 \propto 1/r$, and J_{20} and J_{22} are constant in r. The condition that the absolute value of the right-hand side of equation (11) is less than unity leads to

$$r < r_{\rm cr} = \left|\frac{r\omega_0(r)}{\omega_t}\left(\frac{3}{2}J_{20} - 3J_{22}\right)\right|\,.$$

In Figure 11, we show the solution of equation (11) for the parameters corresponding to model TF, and find that it is consistent with the numerical result of model TF.

VI. DISCUSSION

We investigate gas motion in tumbling prolate and triaxial potentials and confirm the presence of the preferred planes which are predicted from the studies of precession trajectories (Tohline, Simonson, and Caldwell 1982; Durisen *et al.* 1983; Steiman-Cameron and Durisen 1984), except for the preferred plane for the prograde gas ring normal to the tumbling axis. Mulder (1983) found tilted prograde stable orbits in the tumbling potential, but we cannot confirm Mulder's orbits to be preferred planes for gas. This indicates that the conditions for gas to settle into Mulder's stable orbits are rather restricted or that Mulder's stable orbits do not constitute preferred planes for gas. This result indicates that the mechanism for settling gas into Mulder's stable orbits needs to be clarified. Lake and Norman (1983) also found tilted prograde stable orbits.

As summarized in §§ III and IV, in tumbling prolate or triaxial potentials, some retrograde gas rings settle into tilted, warped, preferred planes. If the tumble axis of the potential is the shortest axis of the potential, an inner part of the tilted, warped preferred plane is nearly perpendicular to the longest axis of potential. On the other hand, prograde gas rings are disturbed in elongated prolate potentials, and some part of the gas ring concentrates into the galactic center. Retrograde gas rings normal to the tumble axis in prolate and triaxial potentials are unstable, and the gas concentrates into the galactic center. These results are important in that they suggest a mechanism to supply gas to active galactic nuclei.

The time scale for gas to settle into the preferred plane is the time during which each part of gas ring becomes wound up due to differential precession. This time scale depends on the initial direction of the angular momentum vector of the gas ring, the degree of distortion of the potential, and the fluctuation of angular momentum in each part of the gas ring.

Many polar ring galaxies are observed (Schweizer, Whitemore, and Rubin 1983; Wakamatsu and Arp 1983; Schechter *et al.* 1984; Athanassoula and Bosma 1985). In most of them, polar rings are slightly tilted and warped (Whitemore 1984). For example, NGC 2696 and II Zw 73 have prograde gas rings, and UGC 7576, NGC 4650A, and A0136−0801 have retrograde gas rings.

If the potential of the polar ring galaxy is spherically symmetric, the polar ring is stable. The spherical potential permits the presence of various tilted gas rings. Since all orientations of tilted gas rings are not observed, the possibility of a spherical potential for the polar ring galaxy may be excluded. If the polar ring is formed in a tumbling or nontumbling aspherical potential, our numerical results show that a tilted, prograde gas ring is unstable in a tumbling potential, and that a retrograde gas ring settles into the tilted preferred plane. Therefore, prograde polar rings should be transient. It is important to investigate whether or not the properties of polar rings depend on prograde or retrograde sense of rotation.

The authors thank Professor S. Sakashita for his continous encouragement. We also thank R. H. Durisen for critically reading our manuscript. The numerical calculations were performed at the Computer Center of Hokkaido University. This work was partly supported by Grant-in-Aids for Encouragement of Young Scientists from the Ministry of Education, Science, and Culture (61740135).

REFERENCES

Athanassoula, E., and Bosma, A. 1985, *Ann. Rev. Astr. Ap.*, **23**, 147.
Binney, J. 1978, *M.N.R.A.S.*, **183**, 779.
———. 1981, *M.N.R.A.S.*, **196**, 455.
———. 1982, *Ann. Rev. Astr. Ap.*, **20**, 399.
David, L. P., Steiman-Cameron, T. Y., and Durisen, R. H. 1985, *Ap. J.*, **295**, 65.
de Zeeuw, T., and Merrite, D. 1983, *Ap. J.*, **267**, 571.
Durisen, R. H., Tohline, J. E., Burns, J. A., and Dobrovolskis, A. R. 1983, *Ap. J.*, **264**, 392.
Gingold, R. A., and Monaghan, J. J. 1977, *M.N.R.A.S.*, **181**, 375.
———. 1982, *J. Comput. Phys.*, **46**, 429.
———. 1983, *M.N.R.A.S.*, **204**, 714.
Habe, A., and Ikeuchi, S. 1985, *Ap. J.*, **289**, 540.
Hawarden, T. G., Elson, A. W., Longmore, A. J., Tritton, S. B., and Corwin, H. G., Jr. 1981, *M.N.R.A.S.*, **196**, 747.
Heisler, J., Merritt, D., and Schwarzschild, M. 1982, *Ap. J.*, **258**, 490.
Illingworth, G. 1977, *Ap. J. (Letters)*, **218**, L43.
Lake, G., and Norman, C. 1983, *Ap. J.*, **270**, 51.
Leach, R. 1981, *Ap. J.*, **248**, 485.
Lucy, L. B. 1977, *A.J.*, **80**, 1013.
Magnenant, P. 1982, *Astr. Ap.*, **108**, 89.
Merritt, D., and de Zeeuw, T. 1983, *Ap. J. (Letters)*, **267**, L19.
Mulder, W. A. 1983, *Astr. Ap.*, **121**, 91.
Mulder, W. A., and Hooimeyer, J. R. A. 1984, *Astr. Ap.*, **134**, 158.
Richstone, D. O. 1980, *Ap. J.*, **238**, 103.
Schechter, P. L., Sancisi, R., van Woerden, H., and Lynds, C. R. 1984, *M.N.R.A.S.*, **208**, 111.
Schwarzschild, M. 1982, *Ap. J.*, **263**, 599.
Schweizer, F., Whitmore, B. C., and Rubin, V. C. 1983, *A.J.*, **88**, 909.
Sharples, R. M., Carter, D., Hawarden, T. G., and Longmore, A. J. 1983, *M.N.R.A.S.*, **202**, 37.
Simonson, G. F., and Tohline, J. E. 1983, *Ap. J.*, **268**,.638.
Steiman-Cameron, T. Y., and Durisen, R. H. 1984, *Ap. J.*, **276**, 101.
Tohline, J. E., and Durisen, R. H. 1982, *Ap. J.*, **257**, 94.
Tohline, J. E., Simonson, G. F., and Caldwell, N. 1982, *Ap. J.*, **252**, 92.
van Albada, T. S., Kotanyi, C. G., and Schwarzschild, M. 1982, *M.N.R.A.S.*, **198**, 303.
Wakamatsu, K., and Arp, H. C. 1983, *Ap. J.*, **273**, 167.
Whitmore, B. C. 1984, *Ap. J.*, **287**, 66.
Williams, T. B., and Schwarzschild, M. 1979*a*, *Ap. J.*, **227**, 56.
———. 1979*b*, *Ap. J. Suppl.*, **41**, 209.
Wood, D. 1981, *M.N.R.A.S.*, **194**, 201.

A. HABE: Department of Physics, Hokkaido University, Sapporo 060, Japan

S. IKEUCHI: Tokyo Astronomical Observatory, University of Tokyo, Mitaka 181, Japan